RESEARCH ARTICLE | JULY 10 2006

Magnetoresistance of spin valve structures based on the full Heusler alloy Co_2MnSi

L. J. Singh; C. W. Leung; C. Bell; J. L. Prieto; Z. H. Barber

J. Appl. Phys. 100, 013910 (2006)
https://doi.org/10.1063/1.2213352

Magnetoresistance of spin valve structures based on the full Heusler alloy Co_2MnSi

L. J. Singh,[a] C. W. Leung,[b] C. Bell,[c] J. L. Prieto,[d] and Z. H. Barber
Department of Materials Science and Metallurgy, University of Cambridge, Pembroke Street, Cambridge CB2 3QZ, United Kingdom

(Received 27 July 2005; accepted 15 May 2006; published online 10 July 2006)

Co_2MnSi/Cu/Co pseudo-spin-valves (PSVs) have been grown by dc magnetron sputtering from elemental targets onto GaAs(001). The stoichiometric Heusler layer was highly textured, following the [001] orientation of the lattice matched GaAs(001). Hysteresis loops showed independent switching of the magnetization of the two ferromagnetic layers. Transport measurements of the samples were performed in both the current in plane (CIP) and current perpendicular to plane (CPP) geometries. Clear low-field spin valve contributions were observed at 15 K for the CIP PSV, a conventionally patterned mesa CPP device and a CPP device fabricated in the focused ion beam microscope. Analysis of the CPP data did not show the half-metallic behavior of Co_2MnSi as expected from theory. © *2006 American Institute of Physics*. [DOI: 10.1063/1.2213352]

INTRODUCTION

Half-metallic ferromagnets (HMFs) have attracted increasing interest because of their 100% spin polarized conduction electrons. These materials have great potential in a range of applications, including spin injection into semiconductors.[1] Such materials should also show an enhanced magnetoresistive (MR) response when embedded in heterostructures either as conventional or pseudo-spin-valves (PSVs) utilizing normal metal or tunnel barriers between the ferromagnetic (F) layers, or as spin torque devices (current induced switching of the F layers).[2,3] Heusler alloys are promising candidates for enhancing the MR due to their predicted high spin polarization. The full Heusler alloy Co_2MnSi is one of the most promising spintronic injector materials. It has been predicted to be a HMF (Ref. 4) and crystallizes in the $L2_1$ structure (space group $Fm3m$), which consists of four interpenetrating face-centered-cubic (fcc) sublattices.[5] It is predicted to have a large energy gap in the minority band of ~0.4 eV (Ref. 6) and has the highest Curie temperature amongst the known Heuslers of 985 K.[7]

Films of the Heusler alloy Co_2MnSi have previously been incorporated into tunnel junctions exhibiting a tunneling magnetoresistance (TMR) of 86% at 10 K.[8] However, no MR has been observed in bulk single crystals of Co_2MnSi,[9,10] and to date no PSVs employing this Heusler alloy have been fabricated. Bulk polycrystalline compacts of $Co_2Cr_{0.6}Fe_{0.4}Al$ were found to exhibit a large negative MR of 30% at room temperature, and PSVs utilizing $Co_2Cr_{0.4}Fe_{0.6}Al$ as the bottom electrode showed a maximum giant magnetoresistance (GMR) of 12% at 20 K in the current in plane (CIP) geometry.[11] PSVs with the half Heusler NiMnSb exhibited a current perpendicular to plane (CPP) GMR of 9% at 4.2 K.[12] However, other structures using half metals have shown less promising resistance versus magnetic field $R(H)$ characteristics with MR values around 1% at 60 K for CIP NiMnSb spin valves[13] and $<0.05\%$ at 300 K for CIP and CPP spin valve structures based on Fe_3O_4.[14,15]

In this work we describe the fabrication and measurement of PSV structures utilizing the Heusler alloy Co_2MnSi as the free layer and Co as the harder layer, using the CIP and CPP geometries. We have used both conventional optical lithography (also used for the CIP device) and multilevel processing to form micron-scale CPP mesas, as well as a focused ion beam (FIB) three-dimensional etching technique to access submicron length scales.

EXPERIMENT

The Co_2MnSi/Cu/Co spin valve structures were fabricated *in situ* by dc magnetron sputtering. The Co_2MnSi Heusler layer was deposited from three elemental targets onto GaAs(001) positioned directly below the targets on a Ta strip heater. The geometry of the deposition system is described in earlier work.[16] The substrates were chemically cleaned prior to loading into the vacuum system. The base pressure of the growth chamber was 2×10^{-9} Torr. The substrates were annealed at 868 K for 10 min to remove the native oxide and to obtain the 4×2 surface reconstruction. The temperature was then lowered to the growth temperature of 647 K and the system was pumped for 90 min to ensure complete removal of As, since Mn_2As forms readily at the growth temperature. The Heusler was grown in an argon pressure of 24 mTorr and the deposition rate was 0.1 nm/s. Details of the optimization and properties of the Heusler layer can be found elsewhere.[17] The substrates were then cooled (~280 K) before depositing the Cu layer to minimize interdiffusion. The Cu layer was deposited at 8 mTorr (deposition rate, 0.09 nm/s) followed directly by the Co layer at an argon pressure of 24 mTorr (deposition rate, 0.03 nm/s). Each spin valve structure was capped with at least 4 nm Cu to prevent

[a]Electronic mail: ljl26@cam.ac.uk
[b]Present address: Department of Applied Physics, Hong Kong Polytechnic University, Kowloon, Hong Kong.
[c]Present address: Kamerlingh Onnes Laboratory, Universiteit Leiden, Leiden, The Netherlands.
[d]Present address: Instituto de Sistemas Optoelectronics y Microtecnologia, Avenida Complutense s/n, Madrid 28040, Spain.

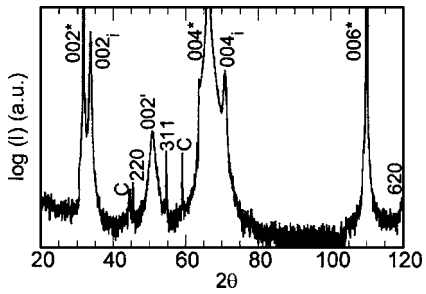

FIG. 1. XRD pattern of the unpatterned $Co_2MnSi(80\ nm)/Cu(5\ nm)/Co(40\ nm)/Cu(4\ nm)$ spin valve structure. Diffraction peaks labeled with "*" denote substrate peaks, "i" are interface peaks, and "′" indicates a combined Cu and Co peak. The sharp lines indexed with a C are W contamination lines from the x-ray tube.

oxidation of the Co layer. Film thickness was determined using profilometry of a lithographically produced step by atomic force microscopy.

For the CIP devices the films were patterned to $20 \times 4\ \mu m^2$ tracks (together with appropriate wiring and contact pads for electrical characterization) with optical lithography followed by broad beam Ar ion milling ($1\ mA\ cm^{-2}$, 500 V). For the first CPP device described, the same method was used, followed by processing with a Ga FIB to achieve vertical transport with a device area of $0.35\ \mu m^2$. This fabrication process with the Ga beam is described in detail elsewhere[18] and has been used previously in the fabrication of all metallic CPP spin valves.[19] This method of fabrication allowed the whole device heterostructure (including thick top electrode) to be deposited *in situ*, giving high quality interfaces. For the second CPP device, conventional Ar ion milling was used to form a $5 \times 5\ \mu m^2$ mesa, followed by the lift-off of a silica insulation layer and finally a top Cu wiring layer, to form a cross geometry.

The generic structure of the spin valves was therefore $Co_2MnSi/Cu/Co/Cu$. The thicknesses of the layers for the CIP film were 10/4/10/2 nm, respectively, 300/10/16/300 nm for the FIB fabricated CPP structure and 80/5/40/4 nm for the conventionally patterned mesa CPP device. For all cases, despite the changes in the coercive field H_c of the Co_2MnSi layer with thickness, the Heusler layer is the free layer in the PSVs.

Film compositions were determined by energy dispersive x-ray analysis in a scanning electron microscope with a precision of 1.5%. Structural characterization was performed by x-ray diffraction (XRD) using Cu $K\alpha$ radiation. The magnetic properties were determined using a vibrating sample magnetometer (VSM). The magnetic field dependence of the resistance $[R(H)]$ was measured using a standard four-point geometry, and the MR was defined as $100\%\ (R\text{-}R_{max})/R_{max}$.

RESULTS AND DISCUSSION

The XRD pattern of the $Co_2MnSi(80\ nm)/Cu(5\ nm)/Co(40\ nm)/Cu(4\ nm)$ unpatterned spin valve structure is shown in Fig. 1. The (002), (004), and (006) peaks from the GaAs substrate can be clearly seen but only very weak peaks from the Co_2MnSi phase. The stoichiometric Heusler layer is highly textured, following the [001] orientation of the lattice matched GaAs(001). However, the (002) and (004) peaks from the Heusler layer can only be resolved by high resolution XRD owing to the very low mismatch with the substrate, as discussed in more detail in another report.[17] The intense (002) and (004) peaks labeled with an "i" originate from an epitaxial interfacial reaction zone between the substrate and the Co_2MnSi, as has been confirmed by high resolution transmission electron microscopy (TEM).[20] The broad peak at 51° is a combined peak of the cold-deposited Cu and Co layers. The layers are still [001] oriented, indicating that they are influenced by the highly oriented Co_2MnSi under layer.

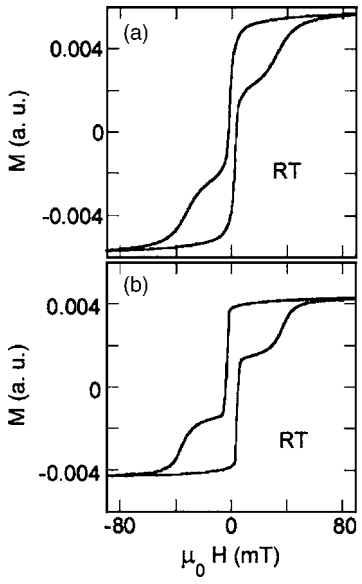

FIG. 2. Hysteresis loops of unpatterned $Co_2MnSi(80\ nm)/Cu(5\ nm)/Co(40\ nm)/Cu(4\ nm)$ at RT in the (a) $[1\bar{1}0]$ (∥ to long axis of chip) and (b) [110] directions.

The magnetic properties of the unpatterned structure illustrated in Fig. 1 were investigated. Hysteresis loops were taken in both the $[1\bar{1}0]$ and the [110] direction, as illustrated in Fig. 2 (directions designated by the wafer manufacturer). It has been observed that plain films of Co_2MnSi do not exhibit the fourfold symmetry expected for a cubic material and the two ⟨110⟩ directions are inequivalent (attributed to the GaAs substrate surface reconstruction).[17] We have generally found that the easy axis of magnetization is in the $[1\bar{1}0]$ direction but occasionally, for unknown reasons the easy axis is in the [110] direction, which is the case here. The hysteresis loop in Fig. 2(a) is not as square as in Fig. 2(b) indicating that for this particular film, the long axis of the chip (∥ to $[1\bar{1}0]$) is actually a semieasy axis. The tracks were patterned along the long axis of the chip, so the devices have not been fabricated in the optimum orientation. However, in both orientations one can clearly see that there is independent switching of the magnetization of the two ferromagnetic layers. In a magnetic field greater than 60 mT the magnetization of the Co and the Co_2MnSi layers is aligned parallel. On reversal of the magnetic field, the magnetization of the Co_2MnSi layer switches first since it has the lower $\mu_0 H_c$ of

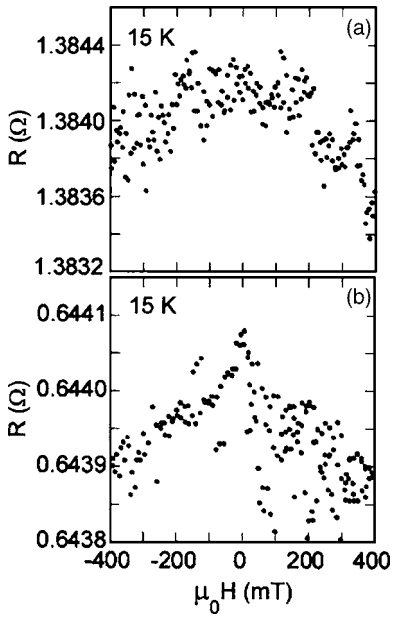

FIG. 3. Magnetoresistance of a 225 nm Co_2MnSi plain film at 15 K in (a) longitudinal configuration and (b) transverse configuration.

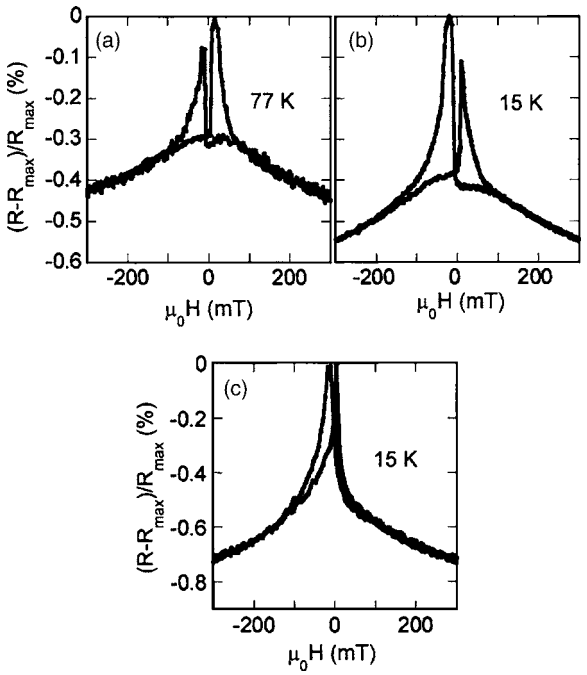

FIG. 4. CIP-MR for Co_2MnSi(10 nm)/Cu(4 nm)/Co(10 nm)/Cu(2 nm) on GaAs(001) spin valve structure. Longitudinal measurements carried out at (a) 77 K and (b) 15 K transverse measurements carried out at (c) 15 K. MR has been normalized to the largest MR at zero field.

2.8 mT, compared to 40 mT for the Co layer, and so the two layers are aligned antiparallel. At larger field the Co layer switches, resulting in the parallel alignment.

Figure 3 shows the resistance of a plain, 225 nm Co_2MnSi film as a function of applied magnetic field at 15 K. In both the longitudinal and transverse configurations the MR is very low ($<0.03\%$) in agreement with bulk single crystals,[9,10] but does not appear to arise from anisotropic magnetoresistance (AMR). In the case of AMR, one would expect a sign change in the R vs H behavior when the orientation of the current and applied field switches from the parallel to perpendicular configuration. The absence of a sign change in Figs. 3(a) and 3(b) indicates no AMR contribution. Similar results have been observed by Hordequin *et al.*[13] in thin films of NiMnSb (300 nm) but not in bulk crystals.

In contrast the CIP spin valve film shows clear peaks in the $R(H)$ curve, associated with the GMR response of the spin valve (Fig. 4). As expected, the MR at 15 K ($\sim 0.45\%$) was higher than at 77 K ($\sim 0.35\%$), and the $R(H)$ measurements with the field parallel and perpendicular to the current flow direction showed a negative MR. In the low-field region (i.e., ±100 mT) there is a difference in the MR behavior in the longitudinal [Figs. 4(a) and 4(b)] and the transverse [Fig. 4(c)] configurations, probably due to the AMR of the Co layer. In addition, there was "background" MR of about 0.1% that persisted even beyond the saturation field. This is similar to what was observed in Fig. 3, although the magnitude is larger here and the difference in the thickness of the Heusler films could account for this.

For the CPP devices, $R(H)$ measurements were also made at 15 K for both the FIB processed device [Fig. 5(a)] and the conventionally patterned mesa structure [Fig. 5(b)]. The MR is $\sim 0.15\%$ for the FIB device, and $\sim 0.35\%$ for the conventionally patterned mesa CPP device, with areal resistance changes $A\Delta R$ (the product of device cross-sectional area and the measured MR change) of 2.4 and 5.6 $\times 10^{-15}\ \Omega\ m^2$, respectively. Since the $A\Delta R$ values are of similar magnitude compared with CPP GMR measurements with $3d$ transition ferromagnets,[21,22] the low MR must arise from the high base resistance in the devices. In this paper MR is defined as the ratio $[\Delta R/R(0)]100\%$, where $R(0)$ is the measured resistance at zero field (or the "base resistance"). For the FIB device this base resistance is coming from the device plus the attached electrodes (refer to Figs. 1 and 2 in Ref. 18 for details), whereas for the mesa it is the

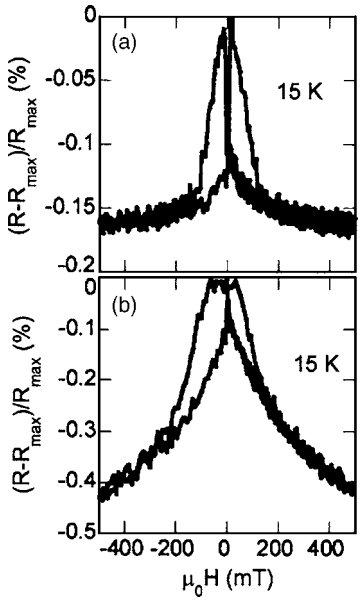

FIG. 5. CPP-MR at 15 K for (a) Co_2MnSi(300 nm)/Cu(10 nm)/Co(16 nm)/Cu(300 nm) on GaAs(001) spin valve structure fabricated using the FIB technique and (b) Co_2MnSi(80 nm)/Cu(5 nm)/Co(40 nm)/Cu(4 nm) on GaAs (001) conventionally patterned spin valve mesa structure.

device resistance plus any contact resistance due to *ex situ* patterning processes. A rough calculation was made using in-house resistivity values measured at 15 K (15, 1, and 40 $\times 10^{-8}$ Ω m for Co, Cu, and Co_2MnSi, respectively). For the FIB device, a reasonable base resistance of ~ 2 Ω was obtained, with a large contribution from the Heusler layer connecting to the device. On the other hand, the calculated base resistance of the lithography patterned mesa device (~ 1.5 mΩ) was far too low to account for the small MR ratio obtained. The extra resistance could possibly come from the interfacial resistance during the patterning process. With suitable optimization of the fabrication process, therefore, we would expect a much higher MR ratio than that obtained here.

For the Heusler alloys that are expected to be HMF, measurements of the spin polarization have yielded values far below the theoretical prediction of 100%.[9,23] Additionally, there has been no attempt to extract the spin diffusion length in such materials. Based on our results and the Valet-Fert (VF) model of CPP GMR,[24] we attempt to estimate the spin diffusion length and the spin asymmetry ratio of Co_2MnSi.

Based on the VF theory, we built a model of the structure Co_2MnSi/Cu (t_{Cu})/Co(t_{Co})/Cu, with infinite thickness for the bottom Heusler and top Cu layers. These assumptions are reasonable for the FIB device, since the electrodes extend over 1 μm from the device layers to the probes. They are questionable for the patterned mesa device since the thickness of the magnetic layers is around 40 nm (this is the actual Co layer thickness, but is just an estimate for the thickness of the Heusler layer participating in the GMR effect in the device, as we have not measured the actual milling depth). Although as we are going to show below, both magnetic layers have a spin diffusion length of the same order of magnitude as that of the magnetic layer thickness in the GMR devices, implying the validity of the modeling results in a qualitative sense. We have neglected any interfacial resistance, since all the layers (in particular, the GMR-active layers and their interfaces) were deposited *in situ*. Whether the interface resistance has to be included depends on its strength relative to the product of resistivity and spin diffusion length of the magnetic layer.[24,25] The major concern here is the Heusler/Cu interface, on which virtually no interfacial resistance information has been reported and we will return to this issue later. With these limitations and assumptions, any resistance change in the multilayer structure should only occur within the Cu spacer. The system is solved by taking into account the conservation of voltages and different spin currents at the interfaces, at the parallel and antiparallel magnetization orientations. The final resistance change is given by the following equation:

$$A\Delta R = \frac{4\beta_{Co}\beta_H \exp(t_{Cu}/l_{Cu})[\exp(t_{Co}/l_{Co})-1]\{[\exp(t_{Co}/l_{Co})+1]\rho_{Co}l_{Co}+[\exp(t_{Co}/l_{Co})-1]\rho_{Cu}l_{Cu}\}}{\alpha\{\exp(2t_{Cu}/l_{Cu})[1+\exp(2t_{Co}/l_{Co})][1+(\rho_{Cu}l_{Cu}/\rho_H l_H)]+\exp(t_{Cu}/l_{Cu})[\exp(2t_{Co}/l_{Co})-1]\}}, \quad (1)$$

where $\alpha = \sinh(t_{Cu}/l_{Cu})[(\rho_{Co}l_{Co}/\rho_{Cu}l_{Cu})+(\rho_{Cu}^2 l_{Cu}^2/\rho_{Co}\rho_H l_{Co} l_H)]+\cosh(t_{Cu}/l_{Cu})[(\rho_{Co}l_{Co}/\rho_H l_H)+(\rho_{Cu}l_{Cu}/\rho_{Co}l_{Co})]$, β refers to the spin asymmetry ratio, ρ is the normalized resistivities of the layers, and l is the spin diffusion length, with subscript H representing the Heusler alloy. We note that as we replace the Heusler layer by Co and when t_{Co} tends to infinity, one can reduce the above result to that of a simple CPP-GMR with two infinite magnetic layers separated by a nonmagnetic spacer [see Eqs. 37 and 45 of Ref. 25].[25] For β_{Co} (0.45), l_{Co} (40 nm), and l_{Cu} (1 μm), we used values obtained from the literature from CPP-GMR measurements.[21,26] A plot of possible combinations of β_H and l_H, using Eq. (1) and the MR data obtained in this experiment, is plotted in Fig. 6. β_H tends asymptotically towards 0.5 for the mesa device and 0.58 for the FIB device. We could not obtain a lower estimate for l_H from the plot, given that it approaches zero when $\beta_H \sim 1$. In common magnetic 3*d* transition metals and alloys the spin diffusion length spans from ~ 5 nm (in $Ni_{80}Fe_{20}$) to ~ 50 nm (in Co) at 4.2 K. A value of $l_H \sim 30$ nm would yield a spin asymmetry of ~ 0.7 for β_H, which is comparable with the other transition metal ferromagnets but still smaller than the value 1 as expected for a HMF. Using an estimate of 4.5 ± 1 fΩ m^2 as obtained from the Heusler/Nb interface,[12] the product of $\rho_H l_H$ (~ 12 fΩ m^2) is about three times the resistance value and the uncertainty in l_H in our estimate can easily cover such a difference. For the case of the Co/Cu interface, the ratio between interfacial resistance to $\rho_{Co}l_{Co}$ is even more dramatic (~ 0.5 vs 6 fΩ m^2).[21] These calculations justify the absence of interfacial resistances in our modeling.

We note that the submicron FIB device shows a much clearer saturation of the resistance at large field, whereas the CIP and mesa structure have a background that is comparable in magnitude with the GMR effect. This kind of background MR has been observed in some reports on GMR superlattices grown by various methods.[27,28] The explanation for such observations is the formation of alloyed interfaces that are (super)paramagnetic, leading to an enhanced scattering of electrons. Alignment of the magnetization in such regions by a large magnetic field can therefore suppress the scattering effect. This is entirely possible at both the GaAs/Co_2MnSi (Ref. 17) and Co_2MnSi/Cu interfaces. Alternatively the observed MR tail could be related to the paraprocess in the saturated regime for the bulk of the magnetic layers, which has been reported in measurements of 3*d* ferromagnetic films under intense field conditions.[29] The differ-

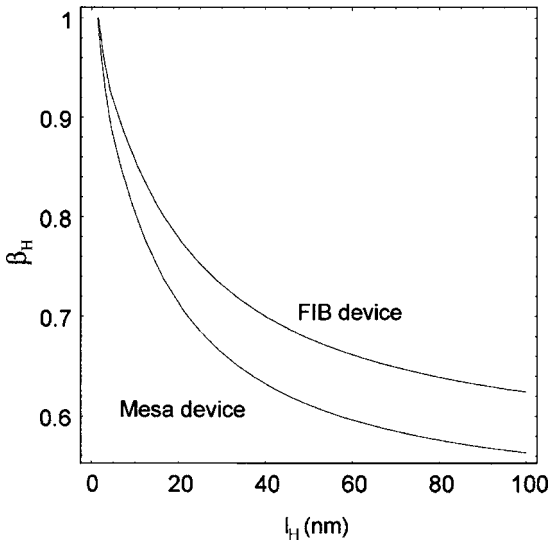

FIG. 6. β_H-l_H plot for the two CPP devices, using Eq. (1) and MR data obtained in this experiment.

ences between Figs. 5(a) and 5(b) may originate from the different growth conditions, thickness of the Heusler layer used, different current flow geometry, or a combination of any of these. More systematic studies are necessary to determine the origin of such a difference: nevertheless the main purpose of this report is to demonstrate the GMR effect in Co_2MnSi-based spin valves, which is clearly shown in Figs. 4 and 5.

CONCLUSION

We have grown and fabricated PSVs of Co_2MnSi/Cu/Co in both the CIP and CPP configurations. Clear low-field spin valve contributions were observed at 15 K for a CIP PSV, conventionally patterned mesa CPP device, and FIB prepared device. The MR values are much lower than that expected from a PSV with a predicted 100% spin polarized electrode. Further optimization of the growth and interfacial conditions, layer thickness, and fabrication process should increase the measured MR.

ACKNOWLEDGMENT

This work was supported by the Engineering and Physical Sciences Research Council, UK.

[1] S. A. Wolf, D. D. Awschalom, R. A. Buhrman, J. M. Daughton, S. von Molnar, M. L. Roukes, A. Y. Chtchelkanova, and D. M. Treger, Science **294**, 1488 (2001).
[2] F. J. Albert, N. C. Emley, E. B. Myers, D. C. Ralph, and R. A. Buhrman, Phys. Rev. Lett. **89**, 226802 (2002).
[3] J. C. Slonczewski, J. Magn. Magn. Mater. **159**, L1 (1996).
[4] S. Ishida, S. Fujii, S. Kashiwagi, and S. Asano, J. Phys. Soc. Jpn. **64**, 2152 (1995).
[5] P. J. Webster, J. Phys. Chem. Solids **32**, 1221 (1971).
[6] S. Ishida, T. Masaki, S. Fujii, and S. Asano, Physica B **239**, 163 (1997).
[7] P. J. Brown, K. U. Neumann, P. J. Webster, and K. R. A. Ziebeck, J. Phys.: Condens. Matter **12**, 1827 (2000).
[8] S. Kammerer, A. Thomas, A. Hutten, and G. Reiss, Appl. Phys. Lett. **85**, 79 (2004).
[9] L. Ritchie *et al.*, Phys. Rev. B **68**, 104430 (2003).
[10] T. Endo, H. Kubota, and T. Miyazaki, J. Magn. Soc. Jpn. **23**, 1129 (1999).
[11] R. Kelekar and B. M. Clemens, Appl. Phys. Lett. **86**, 232501 (2005).
[12] J. A. Caballero, A. C. Reilly, Y. Hao, J. Bass, W. P. Pratt, F. Petroff, and J. R. Childress, J. Magn. Magn. Mater. **199**, 55 (1999).
[13] C. Hordequin, J. P. Nozieres, and J. Pierre, J. Magn. Magn. Mater. **183**, 225 (1998).
[14] H. Takahashi, S. Soeya, J. Hayakawa, K. Ito, A. Kida, C. Yamamoto, H. Asano, and M. Matsui, J. Appl. Phys. **93**, 8029 (2003).
[15] S. van Dijken, X. Fain, S. M. Watts, and J. M. D. Coey, Phys. Rev. B **70**, 052409 (2004).
[16] L. J. Singh, Z. H. Barber, Y. Miyoshi, Y. Bugoslavsky, W. R. Branford, and L. F. Cohen, Appl. Phys. Lett. **84**, 2367 (2004).
[17] L. J. Singh, Z. H. Barber, A. Kohn, A. K. Petford-Long, Y. Miyoshi, Y. Bugoslavsky, and L. F. Cohen, J. Appl. Phys. **99**, 013904 (2006).
[18] C. Bell, G. Burnell, D. J. Kang, R. H. Hadfield, M. J. Kappers, and M. G. Blamire, Nanotechnology **14**, 630 (2003).
[19] C. W. Leung, C. Bell, G. Burnell, and M. G. Blamire, Nanotechnology **15**, 786 (2004).
[20] A. Kohn, A. K. Petford-Long, L. J. Singh, and Z. H. Barber (unpublished).
[21] J. Bass and W. P. Pratt, J. Magn. Magn. Mater. **200**, 274 (1999).
[22] R. D. Slater, J. A. Caballero, R. Loloee, and W. P. Pratt, J. Appl. Phys. **90**, 5242 (2001).
[23] S. F. Cheng, B. Nadgorny, K. Bussmann, E. E. Carpenter, B. N. Das, G. Trotter, M. P. Raphael, and V. G. Harris, IEEE Trans. Magn. **37**, 2176 (2001).
[24] T. Valet and A. Fert, Phys. Rev. B **48**, 7099 (1993).
[25] A. Fert and S. F. Lee, Phys. Rev. B **53**, 6554 (1996).
[26] F. J. Jedema, M. S. Nijboer, A. T. Filip, and B. J. van Wees, Phys. Rev. B **67**, 085319 (2003).
[27] D. Barlett, F. Tsui, D. Glick, L. Lauhon, T. Mandrekar, C. Uher, and R. Clarke, Phys. Rev. B **49**, 1521 (1994).
[28] I. Bakonyi, J. Toth, L. F. Kiss, E. Toth-Kadar, L. Peter, and A. Dinia, J. Magn. Magn. Mater. **269**, 156 (2004).
[29] B. Raquet, M. Viret, E. Sondergard, O. Cespedes, and R. Mamy, Phys. Rev. B **66**, 024433 (2002).